CRATER POPULATION AND RESURFACING OF THE MARTIAN NORTH POLAR CAP. M. E. Banks[1], K. G. Galla[1], S. Bryne[1], B. C. Murray[2], A. S. McEwen[1], and The HiRISE Team, [1]Lunar and Planetary Lab, University of Arizona, Tucson, AZ 85721; mbanks@pirl.lpl.arizona.edu, [2]Geological and Planetary Sciences, California Institute of Technology, Pasadena, CA 91125.

Introduction: The Martian north polar residual cap (NRC) lies on top of the north polar layered deposits (NPLD). The NRC is about 1m thick and composed primarily of large-grained, dust-poor water ice [1]. The mass balance of the north polar cap is uncertain. Satellite imagery reveals small reversible changes in its extent on an interannual basis [2]. Images with a pixel scale of up to 0.25 m/pixel from the High Resolution Imaging Science Experiment (HiRISE) aboard the Mars Reconnaissance Orbiter (MRO), show brighter, or smaller-grained, (i.e. younger) ice superposing darker, or larger-grained, (i.e. older) ice. The lack of dust accumulation indicates that the material composing the NRC accumulated recently. On the other hand, the exposure of darker, larger-grained ice indicates a current state of net ablation. Small pits observed in HiRISE imagery resemble suncups and also suggest recent ablation.

The NPLD are believed to preserve a record of seasonal and climatic cycling of atmospheric water and dust and could reveal important information regarding Martian geologic and climatic history. The NRC is often considered new NPLD material. Thus, understanding the NRC's current behavior and mass-balance in relation to the current climate is an important step in reading the climatic record of the NPLD. One way to do this is to analyze the cratering record of the NRC. Previous studies concluded a NPLD resurfacing age of only ~20-100 Kyr. [3; 4]. However, due to the low resolution of available imagery, these conclusions were based on 0 or 2 craters respectively. To date, data from the Context Camera (CTX) aboard the MRO provide almost complete coverage of the NRC and NPLD with pixel scales of ~5 m/pixel (Figure 1A). To constrain the processes and rates of NRC resurfacing, we are conducting a search for craters within the CTX dataset. Using the NRC crater population data, we will use landscape evolution modeling to investigate the recent (10-100 Kyr) mass-balance history of the NRC.

CTX Search: CTX products available on the Planetary Data System (PDS) are projected using ISIS (Integrated Software for Imagers and Spectrometers) [5] and the crater search is being conducted using ArcMap, a component of ESRI's ArcGIS Geographical Information System (GIS) [6]. To date, ~100 craters have been counted and measured on the NRC and NPLD combined (of which only 4 were previously known); ~70 of these craters are located on the NRC (Figure 1). HiRISE images have been acquired to follow up on 52 of the craters (several in stereo). NRC and NPLD craters range in diameter from ~10-450m (~10–212m for craters on the NRC only). Comparisons of diameters measured in HiRISE and CTX images indicate that our CTX measurements slightly overestimate diameters (Figure 2). The results of the comparison were used to systematically correct CTX-only diameter measurements.

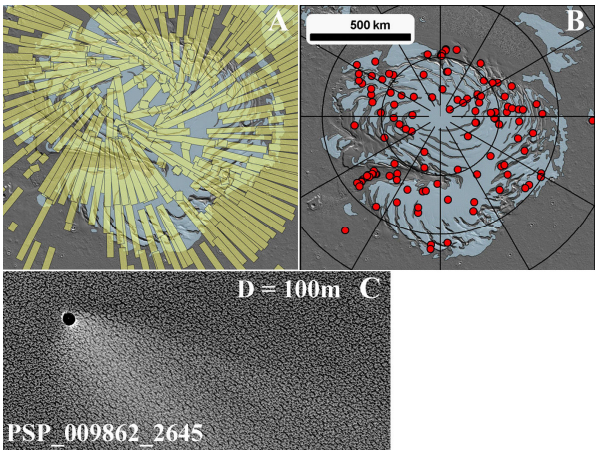

Figure 1: A) Distribution of CTX footprints (yellow polygons) showing CTX coverage of the NRC and NPLD. B) Red dots indicate the locations of craters identified in CTX images. The NRC is highlighted in blue. C) Many craters are easily located due to bright wind streaks (HiRISE image PSP_009862_2645).

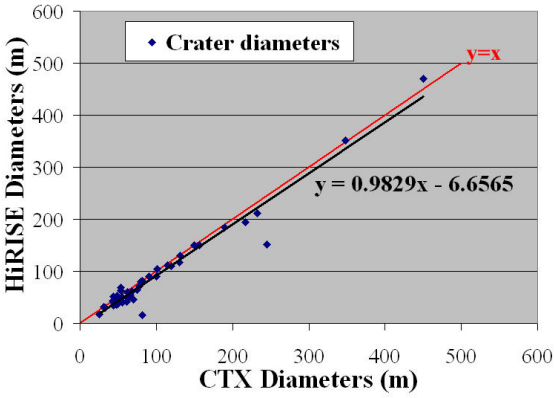

Figure 2: Comparison of crater diameters measured on CTX and HiRISE images showing that CTX measurements slightly overestimate diameters.

Population Statistics: A differential size-frequency distribution plot of the NRC craters was created using HiRISE and corrected CTX diameter meas-

urements (Figure 3). A size-frequency slope of -1.98 was fit over the diameter range 36-150m. The diameter range was selected due to poor statistics in the largest crater size and due to the texture of the NPLD and resolution effects in CTX images which make it difficult to resolve and identify craters <36m in diameter (detection threshold). Variations in slope over the 36-150m diameter range are most likely due to statistical uncertainty. Size-frequency plots can provide insight into an age for a 'production surface' or a resurfacing rate for an 'equilibrium surface.' The Martian production function of combined primary and secondary impact craters is expected to have a slope that is roughly -3.2 in this diameter range and affected by atmospheric screening of projectiles [7]. Since the NRC surface is very young, all craters are probably primary impacts. Thus the differential size-frequency distribution of NRC craters indicates that either the primary production has a lower size-frequency slope than the combined primary and secondary production or that the NRC craters represent an equilibrium population in which many craters have been erased. Based on the wide range in degradation observed in NRC craters (discussed below), we favor the latter and interpret the NRC to be an equilibrium surface with crater lifetime proportional to ~D^(1.2).

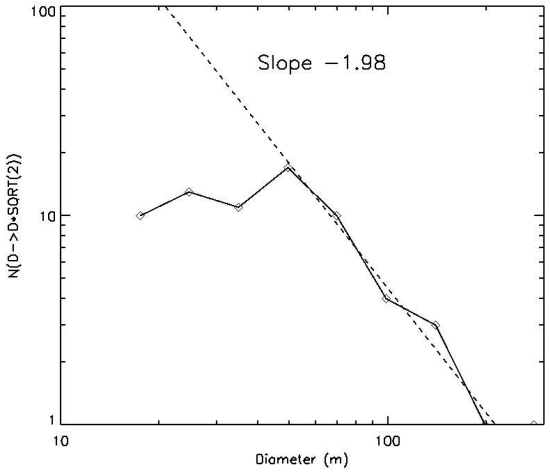

Figure 3: Differential size-frequency distribution plot of NRC craters using HiRISE and corrected CTX diameter measurements. A slope of -1.98 was fit over the diameter range 36–150m.

Crater Degradation and Removal: HiRISE observations reveal a morphological sequence of crater degradation states that provides a qualitative understanding of the processes involved in crater removal (Figure 4). Depth/diameter ratios calculated from shadow measurements for 20 craters range from 0.02 (mostly infilled) to 0.23 (fresh craters) with more than half of the craters having ratios below 0.12. Impact craters are the sites of preferential ice accumulation which gradually infills the crater cavity; shadowing inside the crater promotes accumulation of fresh, small-grained ice which is brighter, stays cooler, and creates a positive feedback. Ablation and eolian erosion also contribute to crater removal by degrading crater rims; ablation pits (suncups) are commonly observed.

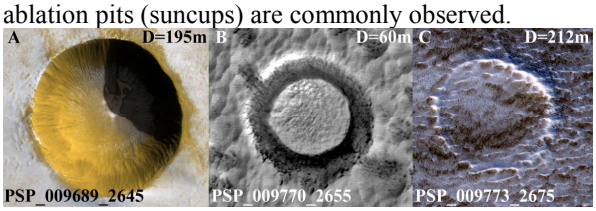

Figure 4: HiRISE images show craters in various stages of degradation. A) A relatively fresh crater with little ice accumulation and rim erosion. B) The floor of the crater has been completely covered by ice accumulation and the rim has been eroded by ablation and wind action. C) The crater is almost completely infilled and the rim is highly degraded.

Modeling Polar Cap Resurfacing: To infer past climatic conditions from the NPLD, we need to connect the current behavior of these deposits to the current climate. Resurfacing of the north polar cap is not directly tied to the crater removal rate as craters are preferred sites for new deposition. However, craters make ideal control features as they constrain rates of processes. The full range of crater morphologies observed in HiRISE images allows "space-for-time" substitution. Variations in the argument of perihelion will have affected polar climate over the lifetime of these craters. When perihelion occurs in the northern summer, as last happen 21,500 Kyr ago [8], icy material may be ablated from the NPLD. Simulations suggest that several meters of ice may have been removed [9] which would be sufficient to remove craters 10s of meters across. We are beginning landscape evolution modeling of accumulation, ablation and eolian redistribution of ice to modify craters. By combining recent orbital solutions [8] with these processes, we can create landscape evolution models that are constrained by the size-frequency and degradation of the observed crater population and can quantifiably investigate the recent (10-100 Kyr) mass-balance history of the NRC. The current crater population is estimated to have accumulated in ~10^4 years.

References: [1] Langevin Y. et al. (2005) *Science, 307,* 1581. [2] Byrne S. et al. (2008) *Planet. Space Sci*., *54*, 194-211. [3] Herkenhoff K. E. and Plaut J. J. (2000) *Icarus*, *144*, 243–253. [4] Tanaka K. L. (2005) *Nature*, *437*, 991-994. [5] http://isis.astrogeology.usgs.gov/ [6] http://www.esri.com/ [7] Hartmann W. K. (2005) *Icarus*, *174*, 294-320. [8] Laskar J. A. et al. (2004) *Icarus*, *170*, 343-364. [9] Montmessin F. et al. (2007) *JGR*, *112*.